Standard Operation Procedure for Continuous Flow Abiotic Dissolution & Transformation Testing of Nanomaterials

Johannes Keller & Wendel Wohlleben

BASF SE, Dept. Experimental Toxicology and Ecology, and Dept. Material Physics, 67056

Ludwigshafen, Germany

johannes-georg.keller@basf.com, wendel.wohlleben@basf.com

Measurement of the dissolution, dissolution rate and transformation of nanomaterials in physiological and environmental media.

Scope:

The present SOP specifies an implementation of a Continuous Flow System as described by ISO/TR 19057:2017. A nanomaterial (NM) is held between ultrafiltration membranes and is subjected to a fixed or variable flow-rate over a certain time at a controlled temperature in a physiological or environmental simulant medium. During that time the effluent is collected and analyzed, e.g. with an autosampler (for parallel testing of several flow-cells over several days) or by direct injection (for optimal time resolution on a single flow-cell). The dissolved analyte is quantified preferentially by elemental analysis, especially Inductively coupled plasma- mass spectrometry (ICP-MS) or inductively coupled plasma- optical emission spectrometry (ICP-OES). The solid residues in the filter cell are recovered at the end of the test, and are analyzed via High resolution scanning electron microscopy (HR-SEM) or transmission electron microscopy (TEM) to detect the transformation of the size and shape of the nanomaterials (by NanoDefine protocols of preparation and image analysis, or other prevalidated methods) and optionally to detect also the speciation and surface chemistry (by Selected Area Electron Diffraction (SAD) or X-ray Photoelectron Spectroscopy (XPS) other suitable techniques). The resulting dissolution rates are preferentially given in units of ng/cm²/h and as half-times, as established for physiological biodissolution.(Oberdörster and Kuhlbusch 2018; IARC 2002) The SOP proposes inherent quality control procedures.

Applicability range:

- Aqueous simulant fluids
- Dissolution rates from 0.01 ng/cm²/h to 500 ng/cm²/h with the recommended parameters. (halftimes on the order of days to weeks) (faster processes by optional settings)
- Metal-containing (nano)materials with or without surface coatings, with sizes from 5 nm.

Funding: This SOP was partially supported by nanoGRAVUR (BMBF, 2014 – 2018).

Content

1. Scope

The evaluation of particle solubility is a key element of many integrated testing strategies (Oberdörster and Kuhlbusch 2018; Burden et al. 2017) and of frameworks for categorizing broad classes of materials, such as ENMs, in terms of their physicochemical properties (Arts et al. 2015; Collier et al. 2015; Drew et al. 2017; Godwin et al. 2015; Kuempel et al. 2012; Oomen et al. 2015; Oomen et al. 2018). Methods to assess the equilibrium (or semi-dynamic) solubility of ENM that are suspended in water or physiological buffers are relatively well developed(Avramescu et al. 2016). Continuous Flow Systems are “seen to be the best method of measuring durability in vitro” (ISO/TR19057 2017), and have been extensively validated on the dissolution kinetics of mineral fibers.(Potter and Mattson 1991; Eastes, Potter, and Hadley 2000; IARC 2002; Guldberg et al. 1995; Guldberg et al. 2000; Guldberg 1998) The present SOP describes minor adaptions to match the specifics of NM. The SOP describes a method for the investigation of the dissolution as well as the transformation of nanomaterials in physiological and environmental media, and has been implemented with simulant fluids of pulmonary macrophages lysosomes, of human stomach, of human intestine and with environmental aquatic medium ADaM.

2. Basics

This SOP describes a standard operation procedure for dynamic dissolution as well as the investigation of transformation of nanomaterials. A static system for the determination of dissolution struggles with supersaturation of the ions of the nanomaterial and can often not reproduce the observations of transformation and dissolution in vivo. A report of the ISO organization (ISO/TR19057 2017), therefore recommends a flow system with a continuous flow, consisting of one or several parallel dissolution cell(s), a peristaltic pump and a sufficiently large reservoir with simulated fluids to sustain the flow through the cell(s) for the entire duration of the experiment.

3. Materials and Instruments

3.1 Materials

The following materials are required:

- At least 1 mg of inorganic nanomaterial (see motivation for choice of mass below)
- BOLA three step flow through filter (BOLA Part. No.: N1682-08, Bohlender GmbH, Germany)
- 5 kDa pore size cellulose triacetate membrane ø 47 mm (Sartorius Stedim Biotech GmbH, Goettingen, Germany)
- 0.22 µm pore size DURAPORE® cellulose membrane ø 47 mm (Merck Millipore Ltd., Ireland)
- ø 0.25 mm PharMed® BPT tubing for peristaltic pump (Ismatec, Cole-Parmer Instrument Company LLC., US)
- ø 0.5 mm Polytetrafluoroethylene (PTFE) tubing for connection of cells (Duratec GmbH, Germany)
- ø 4 mm silicone tube for connection of autosampler with waste (Deltalab, S.L., Spain)
- Ultra-high-molecular-weight-polyethylene (UHMWPE) anti-clogging filters
- 350 mL physiological or environmental fluid
- Deionized water

- 16 mm vials with 12 mL Volume
- Gold TEM grid coated with 25 nm amorphous carbon, 3.05 mm diameter

3.2 Instruments

Comparable equipment as the mentioned instrument is required:

- Heating chamber to maintain a steady temperature of up to 37 °C
- Tempered water bath (with a cover to limit the evaporation)
- Peristaltic dispensing pump (Ismatec IP65, IPC or IPC-N pump, Cole-Parmer Instrument Company LLC., US)
- Sample station autosampler (Sample Station PSC-560, Duratec GmbH, Germany) with 4 racks 5x12 Vials (16 mm diameter)
- Benchtop centrifuge with at least 5000 G (Sepatech Labofuge, Heraeus GmbH, Germany)
- Vacuum roughing pump

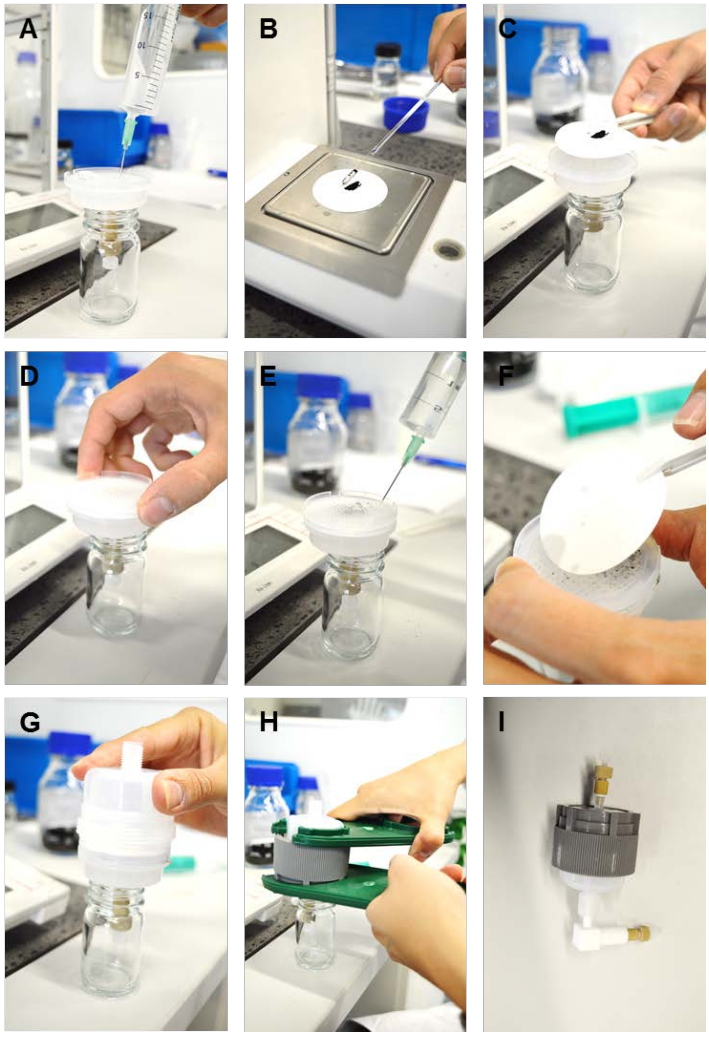

Figure 3.1: Stepwise preparation of the flow-through cell. A, filling of the top part of the cell with medium. B, weighting of the NM directly onto the triacetate cellulose 5 kDa membrane. C, the membrane is transferred onto the cell grid. The second step membrane holder is placed on top of the 5 kDa membrane, step D, and the space between the new grid and the cell is filled with medium, step E. Afterwards the 0.22 µm membrane is placed onto it (F) and the bottom part is attached, G. In step H, the filter is firmly screwed together and closed and afterwards filled with medium. I shows the ready to use flow-through cell.

4. Experimental Procedure

4.1 Flow-through cell preparation

The preparation of the flow-through cell is displayed in ***Figure 4.1.*** The flow-through filter cell is placed upside down in a 30mm glass and closed with a PTFE screw, seen in A. This part of the cell housing is now filled with the desired medium. A defined amount of nanomaterial – here 1 mg – is directly weighted onto the 5 kDa cellulose triacetate membrane and carefully placed on the top part of the cell. The second filter holder is placed on top of the 5 kDa membrane and the space between them is filled with medium. The 0.22 µm membrane is then placed on top of the filter holder, the bottom part is attached and the flow-through cell is closed firmly. Please make sure to not screw the cell too tight together, otherwise the membrane might rupture. Now fill the rest of the cell with medium and close it with a PTFE screw as well.

The stepwise filling procedure (Figure 4.1) was optimized to ensure complete wetting of the membranes, and bubble-free filling of the cell housing. Combined with the pore size of the upper membrane (which has no NM-vs-analyte fractionation task), the hydrostatic pressure of the reservoir (Figure 4.2), the pressure drop across the flow cell membrane remains sufficiently low for reliable operation by peristaltic pumps.

The quality control (section 6) provides criteria to justify the robustness of the results against the choice of the initial NM mass. To prevent supersaturation, one may require that maximally a monolayer of NM should deposit on the membrane. A hypothetical monolayer of 50 nm CeO_2 particles would weigh 0.49 mg on the actual membrane diameter. However, experience shows that the NM redistribute during the experiment, presumably by the flow pattern, so that even very low initial NM mass cannot prevent local concentration gradients. On the other hand, the physical and chemical structure of the NM may change during the experiment, so that a comparison of total dissolved analyte mass vs. initial NM mass is an essential part of the evaluation. Also for the evaluation by a surface-controlled zeroth order dissolution rate (Utembe et al. 2015; ISO/TR19057 2017), the weighing error propagates directly into the dissolution rate. Hence, the initial mass must be accurately measurable on dry NM powders. We recommend 1mg to satisfy all conditions.

Optionally, on may prepare a diluted NM acquous suspension, and let the diluted suspension soak into the membrane, to achieve initial NM masses of 0.1 mg and below, but then one needs to assume that the NM is stable in water.

4.2 Start of the dissolution

Before the start, the flow-rate of the peristaltic pump must be calibrated with a cell that contains all membranes (but no NM) to the desired flow rate – here to 2 mL/h.

To cover the dissolution rates of low or moderately soluble NM, the sampling time points within the autosampler are set to the following values for phagolysosomal simulant fluid (PSF) and environmental fluid: *12h, 24h, 36h, 48h, 60h, 72h, 96h, 120h, 144h, 168h*. The sampling duration

is 5h, and the effluent between samplings is collected in one batch container for each NM, such that no analyte is lost. Optionally for faster processes, one may program non-interrupted 5h-samplings. Optionally for very fast processes, one may inject the effluent directly into the elemental analysis. The sampling time of 5h was chosen to obtain 10mL samples, which is the preferred volume of the local elemental analysis labs, and may be reduced without any impact on the validity of the method.

For gastro intestinal dissolution, the flow rate, as well as the sampling time points need to be adapted to the in vivo exposure durations and conditions. The medium in the reservoir is stored at the desired temperature (37 °C for physiological media, room temperature (RT) for environmental media).

The cell is afterwards connected to the reservoir with PTFE tubing and submerged in the water bath in an upright position. Wait until the first drop leaves the top of the cell, then connect the tubing of the peristaltic pump to the cell. After connecting all the tubes, the dissolution system is ready to be started

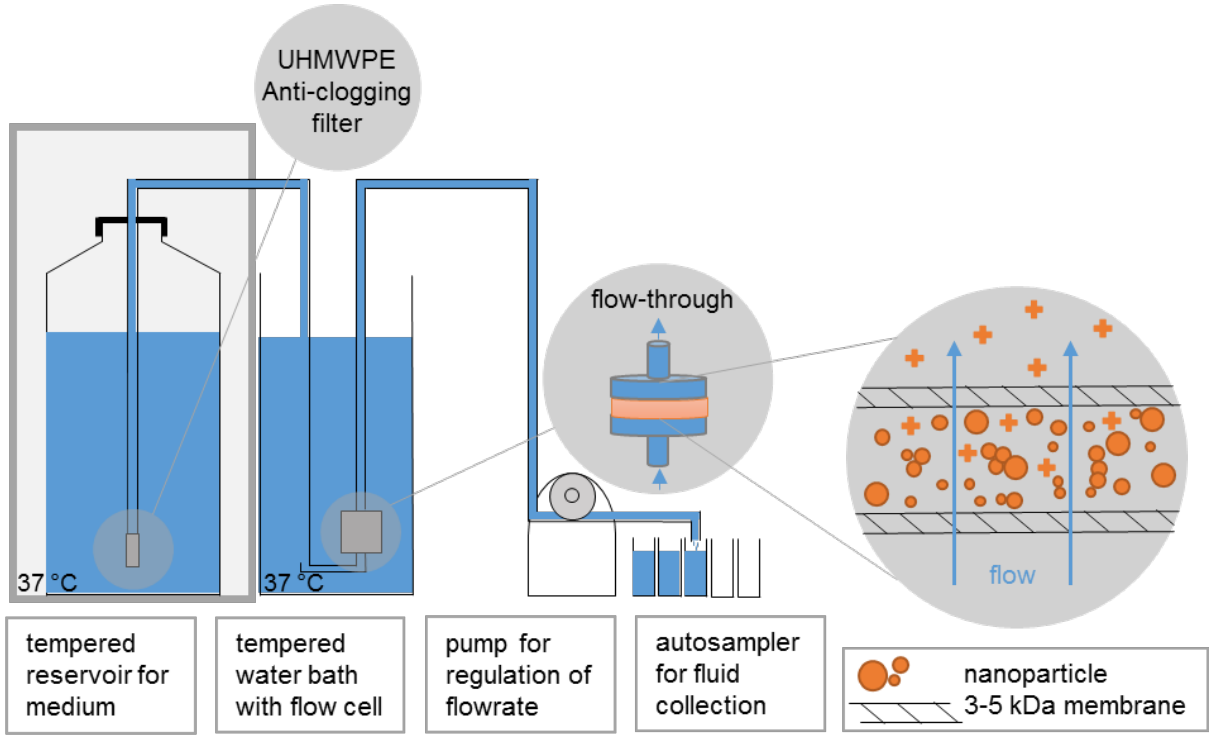

Figure 4.1: Dissolution setup (adapted from (Keller et. al 2018)). The reservoir for the physiological fluid is controlled at 37 °C, as well as the flow-through cells. The peristaltic pump regulates the flow-rate of up to 8 cells in parallel, with a programmable autosampler for fluid collection. The flow-through cell is equipped with a 5 kDa membrane at the top to hold back particles and only allow the flow of ions as recommended by (ISO/TR19057 2017). The meniscus of the reservoir is elevated approx. 0.5m above the cells such that the hydrostatic pressure balances the pressure drop by the 5kDa membrane. If the sampling intervals are non-continuous, the intermittent effluent is collected in a batch for each cell. For clarity, only one cell is shown, but the multi-tube heads of persitaltic pumps easily allow parallel testing of several flow-cells (5 to 8 in the BASF implementation).

4.3 Analysis of effluent

As in agreement with (ISO/TR19057 2017) the sampled vials as well as the batch and the influent medium (to control for elemental background levels and potential matrix interferences) are analyzed for their elementary composition by ICP-OES (Agilent 5100, Agilent, USA) or ICP-MS (Nexion 2000B, Perkin Elmer, USA). It is recommended to detect ions with 0.01 mg/L (10 ppb) limit of quantification, to achieve a lower detection of $k < 0.01$ ng/cm²/h for 1mg initial mass.

4.4 TEM sample preparation

The TEM grid preparation is displayed in ***Figure 4.2*** and consists of multiple steps. The greyish parts are made from PEEK (Polyetheretherketone) at our workshop, whereas the outer centrifuge vial is commercial from forced filtration tubes. Step A, opening of the flow-through cell followed by B rinsing of the remaining nanoparticles from the k5 kDa membrane with Millipore water into a glass. A TEM grid (coated by 25nm amorphous carbon, 3.05 mm diameter) is positioned on the bottom cap and held in place with a ring as shown in C and F, and this detachable bottom is the screwed into the centrifugation tube (C). The solution (3 ml) is then transferred into the centrifugation tubes as seen in C, with a subsequent centrifugation for 2 h at 5000 rpm. Afterwards the solution is removed by unscrewing the TEM grid holder. The droplet on the TEM grid is then soaked up with a tissue, as seen in E. Finally, the TEM grid is left to dry and analyzed. We found that by this method sub-monolayers are formed on the TEM grid.

To dissolve adhering particles and ions between successive uses, the re-usable PEEK parts of the centrifuge equipment were soaked in 1N HNO_3 for 24h. This acid treatment effectively prevented cross-contamination, and was superior to less aggressive washing or sonication procedures.

The evaluation of the TEM results should apply the validated NanoDefine SOP "*Measurement of the minimal external dimension of the primary particles of particulate materials from TEM images by the NanoDefine ParticleSizer software*". This enables a comparison of the number metrics size distribution, and of shape descriptors (roundness etc.) before and after the dissolution experiment.

Optionally, high-resolution SEM can provide an enhanced depth contrast.

Optionally, the speciation can be analyzed by Selected Area Electron Diffraction (SAD) as integrated part of the TEM measurement.

Potentially, surface chemistry may be analyzed by X-ray Photoelectron Spectroscopy (XPS) or other suitable techniques. Of note, the preparation onto the TEM grid by pure-water-washing and centrifugation inherently suppresses dissolved components that may conceal the (transformed) NM surface, but is must be anticipated that molecular layers of the simulant medium remain adherent.

The analysis of the “transformed NM surface” or the loss of functionalization as discussed by ISO TR 19057:2017 is not yet fully established.

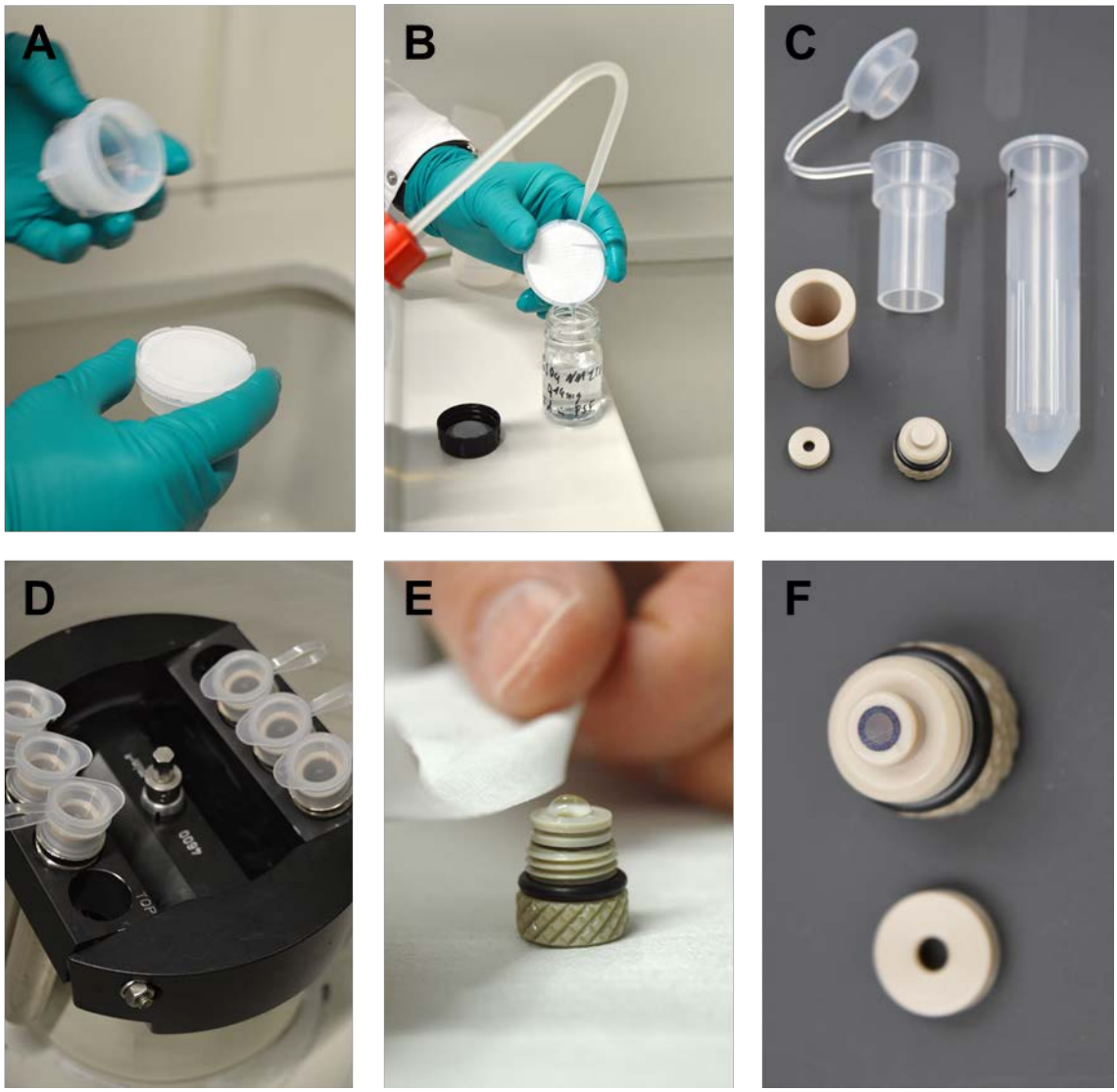

Figure 4.2 Stepwise illustration of the preparation of TEM grid. A opening of the flow-through cell, B Transfer of ENM remnants by rinsing the 5 kDa membrane with Millipore water into a cup or a glass, C Proprietary components of the centrifugation tube. Bottom parts can be unscrewed and were designed to hold a TEM grid in place during centrifugation, D centrifuge with centrifugation tubes. E bottom part after centrifugation: remaining fluid is carefully removed from the particle laden TEM grid. F View on the dry nanoparticle-laden TEM grid (cover ring removed).

5. Calculation of the dissolution

An Excel file for the calculation of the dissolution can be downloaded under: https://www.dropbox.com/sh/649x4flz6figoux/AAAkf4SCoKOUg81zsNG8AF3Ra?dl=0

The interim calculation of the dissolution rate is reproduced here from (Keller et al., 2018), focusing on the cumulated evaluation. If measured kinetics reach 50% dissolution, then the simplest approximation is

$$k = \ln(2)/(BET*t_{1/2}) \quad \text{(Eq. 1)}$$

or, if more than 50% remained at the final time T,

$$k = \ln (M_0 / M_{solids}(T)) / (BET*T), \quad \text{(Eq. 2)}$$

where the mass loss to dissolved matter

$$M_{dissolved}(T) = M_0 – M_{solids}(T) \quad \text{(Eq. 3)}$$

is cumulated from all samplings with concentration c_i, flow V_i and sampling interval Δt_i, and includes the stoichiometry of the detectable ion in the ENM. In a stricter approach, each individual sampling can be evaluated by instantaneous rates: For each sampling interval Δt, the instantaneous dissolution rate k was constructed as

$$k(t) = M_{ion}(t) / SA(t) / \Delta t. \quad \text{(Eq. 4)}$$

Here we approximated the instantaneous surface area

$$SA(t) = BET(t=0) * (M_0 – M_{ion}(t)), \quad \text{(Eq. 5a)}$$

and thus, ignored changes of the size distribution and shape. Alternatively, one can model the loss of solids as the shrinkage of spheres, such that the lost mass is modeled by reduced diameter.

$$SA(t) = BET(t=0) * (M_0 – M_{ion}(t))^{2/3}, \quad \text{(Eq. 5b)}$$

In practice, the differences between rates determined via Eq. 5a and 5b are small, except for the class of highly soluble ENM, but especially for this class, the in-situ TEM (Koltermann-Jülly et al. 2018) casts doubt on the assumption of spherical shape that is needed for Eq. 5b. Overall, we preferred Eq. (4 with 5a) if we investigated dynamic processes for scientific purposes. For grouping purposes, we stick to the simpler Eq. 2.

6. Quality Control

The dissolution rate should not be limited by the chosen parameters of flow rate and initial mass. Specifically, it is the purpose of the continuous flow system to maintain out of equilibrium conditions, and thus to prevent the supersaturation that can occur with static systems, and can inhibit further dissolution (ISO 19057:2017).

To confirm that the dissolution is not limited by supersaturation, on can reduce the initial mass or increase the flow rate V, effectively reducing the ratio SA/V. Optionally, this is implemented by a programmed peristaltic pump that initiates the experiment at flow rates of 0.2 mL/h and increases for successive samplings up to 3mL/h. Higher flows are hard to achieve with 5kDs separation membranes. If the dissolution rate determined by Eq. 4 increases for the samplings obtained at lower SA/V (higher flow rates), this is indication that saturation limited the dissolution at the high SA/V conditions. Supersaturation is thus detected for BaSO4 NM220 in phagolysosomal pH4.5 media, as confirmed by replicate flow-cell dissolution experiments at U. Rochester and at BASF, and in accord with in vivo findings. (Keller et al. 2018, to be submitted_a) However, materials such as CuO (SUN) or SiO_2 NM 203 have constant dissolution rates irrespective of the SA/V conditions. (Keller et al. 2018 to be submitted_b).

7. Validation status and comparison against in vivo studies

The abiotic dissolution rates measured by the present SOP with phagolysosomal simulant fluid (Stefaniak 2005) have been benchmarked against in vivo inhalation for 24 nanoforms of 6 substances. (Koltermann-Jülly et al. 2018) Decadic ranges of dissolution rates matched the NM substance composition and their in vivo pulmonary clearance results.

The present SOP has also been applied to oral testing with simulated gastric fluid (GF) and simulated intestinal fluid (FeSSIF), to explain the different in vivo oral effects of two nanoforms of Cu-based NM via their differences in intestinal biodissolution (Hristozov et al. 2018).

The present SOP has finally been applied to four OECD NM in Aachener daphnia medium (ADaM).

No complications occurred with any of the above media, but the method has been validated by a pilot interlaboratory comparison (Alison Elder, Günter Oberdörster at U. Rochester + BASF) and benchmarking against in vivo results only for the pulmonary compartment.

The composition of each fluid can be found in the supplementary information.(Marques, Loebenberg, and Almukainzi 2011; Stefaniak 2005). The used media are in accordance with the (ISO/TR19057 2017).

This SOP has been used for the dissolution- & transformation-based rationalization of in vivo findings in:

- Johanna Koltermann-Jülly, Johannes G. Keller, Antje Vennemann, Kai Werle, Philipp Müller, Lan Ma-Hock, Robert Landsiedel, Martin Wiemann, Wendel Wohlleben. '*Abiotic dissolution rate of 24 (nano)forms of 6 substances compared to macrophage-assisted dissolution and in vivo pulmonary clearance: Grouping by biodissolution and transformation*', NanoImpact (**2018**) DOI: https://doi.org/10.1016/j.impact.2018.08.005
- Wim H. De Jong, Eveline De Rijk, Alessandro Bonetto, Wendel Wohlleben, Vicki Stone, Andrea Brunelli, Elena Badetti, Antonio Marcomini, Ilse Gosens, Flemming R. Cassee. 2018. '*Toxicity of copper oxide and basic copper carbonate nanoparticles after short-term oral exposure in rats*', Nanotoxicology (**2018**) https://doi.org/10.1080/17435390.2018.1530390
- Johannes G. Keller, Uschi Graham, Johanna Koltermann-Jülly, Robert Gelein, Lan Ma-Hock, Robert Landsiedel, Martin Wiemann, Günter Oberdörster, Alison Elder, Wendel Wohlleben. *'Predicting the dissolution and transformation of inhaled nanoparticles in the lung using abiotic flow cells: The case of barium sulfate', to be submitted (*2018).

8. References

Arts, Josje H. E., Mackenzie Hadi, Muhammad-Adeel Irfan, Athena M. Keene, Reinhard Kreiling, Delina Lyon, Monika Maier, Karin Michel, Thomas Petry, Ursula G. Sauer, David Warheit, Karin Wiench, Wendel Wohlleben, and Robert Landsiedel. 2015. 'A decision-making framework for the grouping and testing of nanomaterials (DF4nanoGrouping)', *Regulatory Toxicology and Pharmacology*.

Avramescu, M.-L., P. E. Rasmussen, M. Chénier, and H. D. Gardner. 2016. 'Influence of pH, particle size and crystal form on dissolution behaviour of engineered nanomaterials', *Environmental Science and Pollution Research*: 1-12.

Burden, Natalie, Karin Aschberger, Qasim Chaudhry, Martin JD Clift, Shareen H Doak, Paul Fowler, Helinor Johnston, Robert Landsiedel, Joanna Rowland, and Vicki Stone. 2017. 'The 3Rs as a framework to support a 21st century approach for nanosafety assessment', *Nano Today*, 12: 10-13.

Collier, Zachary A., Alan J. Kennedy, Aimee R. Poda, Michael F. Cuddy, Robert D. Moser, Robert I. MacCuspie, Ashley Harmon, Kenton Plourde, Christopher D. Haines, and Jeffery A. Steevens. 2015. 'Tiered guidance for risk-informed environmental health and safety testing of nanotechnologies', *Journal of Nanoparticle Research*, 17: 155.

Drew, Nathan M., Eileen D. Kuempel, Ying Pei, and Feng Yang. 2017. 'A quantitative framework to group nanoscale and microscale particles by hazard potency to derive occupational exposure limits: Proof of concept evaluation', *Regulatory Toxicology and Pharmacology*, 89: 253-67.

Eastes, Walter, Russel M. Potter, and John G. Hadley. 2000. 'ESTIMATING IN VITRO GLASS FIBER DISSOLUTION RATE FROM COMPOSITION', *Inhalation Toxicology*, 12: 269-80.

Godwin, Hilary, Catherine Nameth, David Avery, Lynn L. Bergeson, Daniel Bernard, Elizabeth Beryt, William Boyes, Scott Brown, Amy J. Clippinger, Yoram Cohen, Maria Doa, Christine Ogilvie Hendren, Patricia Holden, Keith Houck, Agnes B. Kane, Frederick Klaessig, Toivo Kodas, Robert Landsiedel, Iseult Lynch, Timothy Malloy, Mary Beth Miller, Julie Muller, Gunter Oberdorster, Elijah J. Petersen, Richard C. Pleus, Philip Sayre, Vicki Stone, Kristie M. Sullivan, Jutta Tentschert, Philip Wallis, and Andre E. Nel. 2015. 'Nanomaterial Categorization for Assessing Risk Potential To Facilitate Regulatory Decision-Making', *Acs Nano*, 9: 3409-17.

Gosens, Ilse, Flemming R. Cassee, Michela Zanella, Laura Manodori, Andrea Brunelli, Anna Luisa Costa, Bas G. H. Bokkers, Wim H. de Jong, David Brown, Danail Hristozov, and Vicki Stone. 2016. 'Organ burden and pulmonary toxicity of nano-sized copper (II) oxide particles after short-term inhalation exposure', *Nanotoxicology*, 10: 1084-95.

Guldberg, M. 1998. 'Measurement of in-vitro fibre dissolution rate at acidic pH', *Annals of Occupational Hygiene*, 42.

Guldberg, Marianne, Vermund R Christensen, W Krøis, and Klaus Sebastian. 1995. 'Method for determining in-vitro dissolution rates of man-made vitreous fibres', *Glass science and technology*, 68: 181-87.

Guldberg, Marianne, Alain de Meringo, Ole Kamstrup, Hans Furtak, and Charles Rossiter. 2000. 'The development of glass and stone wool compositions with increased biosolubility', *Regulatory Toxicology and Pharmacology*, 32: 184-89.

Hristozov, Danail, Lisa Pizzol, Gianpietro Basei, Alex Zabeo, Aiga Mackevica, Steffen Foss Hansen, Ilse Gosens, Flemming R Cassee, Wim de Jong, and Antti Joonas Koivisto. 2018. 'Quantitative human health risk assessment along the lifecycle of nano-scale copper-based wood preservatives', *Nanotoxicology*: 1-19.

IARC, INTERNATIONAL AGENCY FOR RESEARCH ON CANCER. 2002. "MAN-MADE VITREOUS FIBRES." In, 1-433. WORLD HEALTH ORGANIZATION.

ISO/TR19057. 2017. 'Nanotechnologies — Use and application of acellular in vitro tests and methodologies to assess nanomaterial biodurability', *ISO/TR*, 19057.

Keller, J., W. Wohlleben, L. Ma-Hock, V. Strauss, S. Gröters, K. Küttler, K. Wiench, C. Herden, G. Oberdörster, B. Ravenzwaay, and R. Landsiedel. 2014. 'Time course of lung retention and toxicity of inhaled particles: short-term exposure to nano-Ceria', *Arch Toxicol*, 88.

Klüttgen, B, U Dülmer, M Engels, and HT Ratte. 1994. 'ADaM, an artificial freshwater for the culture of zooplankton', *Water research*, 28: 743-46.

Koltermann-Jülly, Johanna, Johannes G. Keller, Antje Vennemann, Kai Werle, Philipp Müller, Lan Ma-Hock, Robert Landsiedel, Martin Wiemann, and Wendel Wohlleben. 2018. 'Abiotic dissolution rates of 24 (nano)forms of 6 substances compared to macrophage-assisted dissolution and in vivo pulmonary clearance: Grouping by biodissolution and transformation', *NanoImpact*.

Konduru, Nagarjun, Jana Keller, Lan Ma-Hock, Sibylle Gröters, Robert Landsiedel, Thomas C Donaghey, Joseph D Brain, Wendel Wohlleben, and Ramon M Molina. 2014. 'Biokinetics and effects of barium sulfate nanoparticles', *Particle and Fibre Toxicology*, 11: 55.

Kuempel, E, V Castranova, C Geraci, and P Schulte. 2012. 'Development of risk-based nanomaterial groups for occupational exposure control', *J. Nanopart Res*, 14: 1029.

Landsiedel, R., L. Ma-Hock, T. Hofmann, M. Wiemann, V. Strauss, S. Treumann, W. Wohlleben, S. Groeters, K. Wiench, and B. Ravenzwaay. 2014. 'Application of short-term inhalation studies to assess the inhalation toxicity of nanomaterials', *Part Fibre Toxicol*, 11.

Marques, MRC, R Loebenberg, and M Almukainzi. 2011. 'Simulated Biological Fluids with Possible Application in Dissolution Testing', *Dissolution Technologies*, 8: 15-29.

Oberdörster, Günter, and Thomas A. J. Kuhlbusch. 2018. 'In vivo effects: Methodologies and biokinetics of inhaled nanomaterials', *NanoImpact*, 10: 38-60.

Oomen, Agnes G, Eric AJ Bleeker, Peter MJ Bos, Fleur van Broekhuizen, Stefania Gottardo, Monique Groenewold, Danail Hristozov, Kerstin Hund-Rinke, Muhammad-Adeel Irfan, and Antonio Marcomini. 2015. 'Grouping and read-across approaches for risk assessment of nanomaterials', *International journal of environmental research and public health*, 12: 13415-34.

Oomen, Agnes G., Klaus Günter Steinhäuser, Eric A. J. Bleeker, Fleur van Broekhuizen, Adriënne Sips, Susan Dekkers, Susan W. P. Wijnhoven, and Philip G. Sayre. 2018. 'Risk assessment frameworks for nanomaterials: Scope, link to regulations, applicability, and outline for future directions in view of needed increase in efficiency', *NanoImpact*, 9: 1-13.

Potter, R. M., and S. M. Mattson. 1991. 'Glass fiber dissolution in a physiological saline solution', *Glastechnische Berichte*, 64: 16-28.
Stefaniak, A. B. 2005. 'Characterization of phagolysosomal simulant fluid for study of beryllium aerosol particle dissolution', *Toxicology in Vitro*, 19.
Utembe, Wells, Kariska Potgieter, Aleksandr Byron Stefaniak, and Mary Gulumian. 2015. 'Dissolution and biodurability: Important parameters needed for risk assessment of nanomaterials', *Particle and Fibre Toxicology*, 12: 11.

9. Supplementary Information

9.1 Composition of Media

9.1.1 PSF

Chemical composition reproduced from (Stefaniak 2005). The fluid has pH 4.5.

Table 1: Chemical composition of phagolysosomal simulant fluid (PSF).

Substance	**[mg/L]**
Sodium phosphate dibasic anhydrous	142
Sodium chloride	6650
Sodium sulfate anhydrous	71
Calcium chloride dehydrate	29
Glycine	450
Potassium hydrogen phthalate	4084.6
Alkylbenzyldimethylammonium chloride	50

9.1.2 GF

Chemical composition reproduced from (Marques, Loebenberg, and Almukainzi 2011). The fasted-state simulated gastric fluid (FaSSGF) fluid has pH 1.6.

Table 2: Chemical composition of simulated gastric fluid FaSSGF.

Substance	
Sodium taurochlorate	80 µM
Lecithin	20 µM
Pepsin	0.1 mg/mL
Sodium chloride	34.2 mM
Hydrochloride acid/ sodium hydroxide q.s.	pH 1.6

9.1.3 ADaM

Chemical composition reproduced from (Klüttgen et al. 1994). The Aachener Daphnia Medium (ADaM) has pH 9.0.

Table 3: Chemical composition of Aachener Daphnia Medium (ADaM).

Substance	
Synthetic sea salt (Wimex hw Meersalz Bioelemente)	0.333 g/L
$CaCl_2$-solution, 0.8 mol/L (117.6 g/L $CaCl_2$ * $2H_20$	2.3 mL/L
$NaHCO_3$-solution, 0.3 mol/L (25.2 g/L $NaHCO_3$)	2.2 mL/L
SeO_2-solution, 0.013 mol/L (1.4g/L SeO_2)	0.1 mL/L

10. ANNEX exemplary results

Table 4: Comparison of 7-day abiotic dissolution (standard conditions) with 28-day clearance in vivo short-term instillation studies (STIS) (reproduced from Koltermann-Jülly et al. 2018).

	Dissolution rate Abiotic flow-through, pH4.5 [ng/cm²/h]	**Half-time calculated from k by $t_{1/2} = \frac{\ln(2)}{BET \cdot k_{diss}}$ [d]**	**Dissolution rate Abiotic flow-through, pH4.5 [% per 7 days]**	**In vivo pulmonary clearance in STIS recovery [% per 21 days]**	**Literature STIS**
$BaSO_4$ NM220	10	7	58 %	52 %	1
CeO2 NM212	< 0.73 (LoD)	> 147	<3 % (LoD)	5 %	2
CuO	283	0.73	100 %	>85 % (LoD)	3
TiO_2 NM105	< 0.013 (LoD)	> 4356	< 0.1% (LoD)	26%	4
ZnO NM110	204	1.18	100%		
ZnO NM111	177	1.17	100 %	93 %	4

[1] (Konduru et al. 2014), [2] (Keller et al. 2014), [3] (Gosens et al. 2016), [4] (Landsiedel et al. 2014)

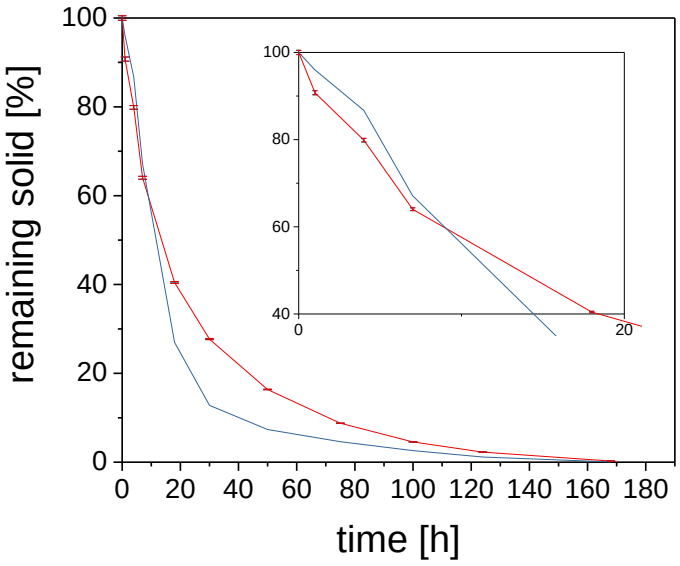

Figure 10.1: Dissolution kinetics of ZnO NM110 (red) and ZnO NM111 (blue) (reproduced from Koltermann-Jülly et al. 2018).

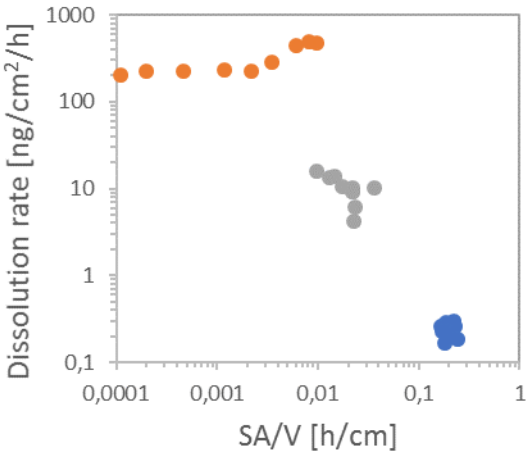

Figure 10.2: Example of a quality control by measuring dissolution rates across a range of different materials $BaSO_4$ NM220 1,05 mg (gray), CuO 1.56 mg (orange), SiO_2 NM203 0,144 mg (blue) and plotting them against SA/V.

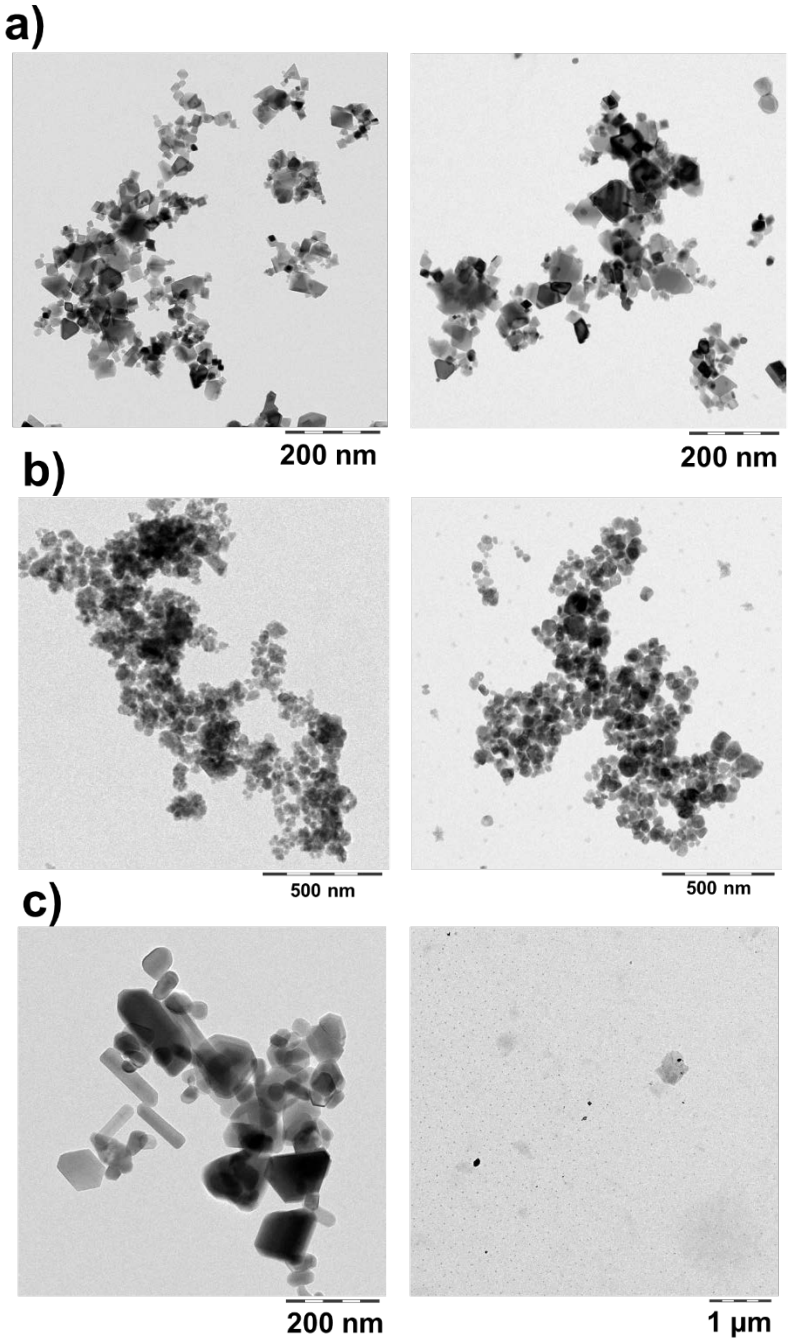

Figure 10.3: TEM images of a) CeO_2 NM212, b) $BaSO_4$ NM220 and c) ZnO NM110 (reproduced from Koltermann-Jülly et al. 2018). Left: before dissolution testing. Right: after 75h dissolution testing in pH4.5 PSF lysosomal simulant.